Diallyl disulphide depletes glutathione in *Candida albicans*:

oxidative stress-mediated cell death studied by two-photon microscopy

Katey M. Lemar[1], **Miguel A. Aon**[2], **Sonia Cortassa**[2], **Brian O'Rourke**[2], **Carsten T. Müller**[1], and **David Lloyd**[1],[*]

[1]*Microbiology (BIOSI 1), Main Building, Cardiff University, PO Box 915, Cardiff CF10 3TL, UK*

[2]*Institute of Molecular Cardiobiology, Johns Hopkins University, 720 Rutland Avenue, 1059 Ross Building, Baltimore, MD 21205-2195, USA*

Abstract

Using two-photon scanning laser microscopy, we investigated the effect of an *Allium sativum* (garlic) constituent, diallyl disulphide (DADS), on key physiological functions of the opportunistic pathogen *Candida albicans*. A short 30 min exposure to 0.5 m$_M$ DADS followed by removal induced 70% cell death (50% necrotic, 20% apoptotic) within 2 h, increasing to 75% after 4 h. The early intracellular events associated with DADS-induced cell death were monitored with two-photon fluorescence microscopy to track mitochondrial membrane potential ($\Delta\Psi_m$), reactive oxygen species (ROS) and NADH or reduced glutathione (GSH) under aerobic conditions. DADS treatment decreased intracellular GSH and elevated intracellular ROS levels. Additionally, DADS induced a marked decrease of $\Delta\Psi_m$ and lowered respiration in cell suspensions and isolated mitochondria. *In vitro* kinetic experiments in cell-free extracts suggest that glutathione-S-transferase (GST) is one of the intracellular targets of DADS. Additional targets were also identified, including inhibition of a site or sites between complexes II-IV in the electron transport chain, as well as the mitochondrial ATP-synthase. The results indicate that DADS is an effective antifungal agent able to trigger cell death in *Candida*, most probably by eliciting oxidative stress as a consequence of thiol depletion and impaired mitochondrial function.

Keywords

garlic; yeast; oxidative stress; mitochondria; membrane potential; respiration; apoptosis; necrosis

Introduction

The opportunistic human pathogen *Candida albicans* is associated with a range of clinical conditions. The organism most commonly disseminates from vaginal and oral mucosal infections to a more complex and life-threatening systemic condition, particularly manifest in immunocompromised patients, such as those suffering from AIDS or undergoing chemotherapy (Cutler, 1991; Odds, 1988). A limited range of anti-fungal treatments is available, but these are often associated with unpleasant side effects. The increasing resistance to favoured treatments using fluconazole or amphotericin necessitates investigations into new treatments for fungal infection.

Decisive breakthroughs in the search for novel antifungal agents will be facilitated by the identification of the most sensitive cellular variables leading to cell death. Oxidative stress,

[*]Correspondence to: David Lloyd, Microbiology (BIOSI 1), Main Building, Cardiff University, PO Box 915, Cardiff CF10 3TL, UK. E-mail: lloydd@Cardiff.ac.uk

associated with elevated reactive oxygen species (ROS), is one of the most sensitive predictors of cytotoxicity in many organisms and cellular systems. Oxidative stress is also a well-established initiator of apoptosis. Cell death is assumed to be triggered as a consequence of cumulative oxidative damage (Poljak *et al.*, 2003). High concentrations of ROS trigger biochemical mechanisms (Halliwell and Gutteridge, 1999) which promote the morphological changes, nuclear fragmentation, chromatin condensation, cellular swelling (blebbing), and membrane remodelling (phosphatidylserine externalization) events associated with the apoptotic route of death (Bowen, 1993; Schwartzman and Cidlowski, 1993; Willie, 1980). These characteristic morphological markers and biochemical changes have been observed in brewer's yeast, *Saccharomyces cerevisiae* (Madeo *et al.*, 1997), although the mechanisms and genetic influences are not well understood.

Death of *C. albicans* is commonly elicited after exposure to environmental and physiological stresses (Del Carratore *et al.*, 2002; Frohlich and Madeo, 2000; Huh *et al.*, 2002; Ludovico, 2001; Madeo *et al.*, 1999, 2002a, 2002b) or in cases such as aged or mutated organisms (Laun *et al.*, 2001; Severin and Hyman, 2002). A demonstration of apoptosis after oxidative stress following exposure to acetic acid and hydrogen peroxide was recently reported for *C. albicans* (Phillips *et al.*, 2003).

Pharmacological properties of plant extracts are well documented and their underlying mechanisms are gradually being understood. Their antimicrobial efficacy may well depend upon the multiplicity of intracellular targets that become inactivated. For *Allium sativum* (garlic), no example of acquired microbial resistance has been reported (Harris *et al.*, 2000; Lawson, 1996); which may stem from its diverse modes of action. Work with *Giardia intestinalis* (Harris *et al.*, 2000) and *C. albicans* (Lemar *et al.*, 2002) suggests that two of the simplest garlic constituents, allyl alcohol (AA) and diallyl disulphide (DADS), are amongst its most potent components. Within mammalian systems, the application of DADS has been successful at inhibiting cell proliferation in human colon, skin and liver tumours (Sundaram and Milner, 1996). More specifically, apoptotic induction by DADS was reported in leukaemia cells via activation of the caspase-3 pathway (Park *et al.*, 2002). Elevated levels of ROS following DADS exposure has been indicated as the primary cause for apoptotic cell death in neuroblastomas (Filomeni *et al.*, 2003).

In this paper we investigate the effects of DADS on cell death in *C. albicans*, with the hope of defining its intracellular targets and mechanisms of toxicity. A main finding is that transient and short exposure to DADS elicits up to 75% cell death within 4 h by either necrosis or apoptosis. The effects of DADS are probably mediated by oxidative stress, and support its potential usefulness in the therapeutic induction of cell death in *C. albicans*.

Materials and methods

Organism and culture

Candida albicans (Berkhout) 5134 was grown in YPD medium [bacto-peptone 2% w/v (Difco, Michigan, USA); yeast extract 1% w/v (Oxoid, Hampshire, UK) and glucose 2% w/v]. An early stationary phase culture was used as an inoculum (1 : 100 dilution in 50 ml) in 100 ml conical flasks. Growth was aerobic at 30 °C in a rotary shaker (150 rev/min). Cell numbers were determined using a haemocytometer slide (Fuschs-Rosenthal, London, UK) after dilution in sterile medium. Optical density (A_{450nm}) was measured using a spectrophotometer (SP-1400; Pye-Unicam, Cambridge, UK). Stock cultures of *C. albicans* were grown overnight at 30 °C and maintained at 4 °C on YPD agar containing 2% w/v agar (Oxoid).

Materials

TMRE, CM-H$_2$DCFDA and monochlorobimane were purchased from Molecular Probes (OR, USA). All other reagents, including enzymes, were from Sigma-Aldrich unless specified. Garlic Powder was from Cultech Biospeciality Products (Swansea, UK).

Garlic preparations

Garlic powder (GP; provided by Cultech Biospeciality Products, Swansea, UK) was prepared to the required concentration (w/v) in sterile medium and placed at room temperature for 30 min. The extract was centrifuged at $3900 \times g$ for 10 min and the supernatant fluid passed through a sterile 0.2 μm filter (Millipore, Watford, UK). Stock solutions of 40 mg/ml were prepared on the same day of testing. DADS was prepared in DMSO and AA in PBS, pH 5.6.

Redox investigation: pre-incubation and conditions for microscopic examination

Early stationary phase cells were harvested and resuspended in PBS, pH 5.6. Samples (0.5 ml) were preloaded with 200 nM TMRE at 37 °C for 30 min before sample removal to the observation chamber and supplemented with 10 m$_M$ glucose. The dish containing the yeasts was equilibrated with unrestricted access to atmospheric oxygen on the stage of a Nikon E600FN upright microscope, which was maintained at 30 °C.

Fluorescent probes for two-photon laser scanning microscopy

The cationic potentiometric fluorescent dye, TMRE, was used to monitor changes in $\Delta\Psi_m$. The large potential gradient across the inner mito-chondrial membrane results in the accumulation of TMRE within the matrix compartment, according to its Nernst potential (Loew *et al*., 1993). ROS production was monitored with the ROS-sensitive fluorescent probe 5-(-6)-chloromethyl-2′, 7′-dichlorohydrofluorescein diacetate (CM-H$_2$ DCFDA, 10 μ$_M$). The acetate group of CM-H$_2$ DCFDA is hydrolysed by esterases when it enters the cell and is trapped inside as the non-fluorescent 5-(-6)-chloromethyl-2′, 7′-dichlorohydrofluorescein (CM-H$_2$DCFH). CM-H$_2$DCFH was chosen because, unlike underivatized dichlorohydrofluorescein, it is well retained in cells (Xie *et al*., 1999) and, in our case, in the mitochondrial matrix (Aon *et al*., 2003). Oxidation of CM-H$_2$DCFH by ROS, particularly by hydrogen peroxide (H$_2$O$_2$) and hydroxyl radical (Vanden Hoek *et al*., 1997), yields the fluorescent product CM-DCF and, in an indirect manner, measures mitochondrially-produced O$_2^{.-}$ that has dismutated to H$_2$O$_2$ through the action of superoxide dismutase (Chance *et al*., 1979; Turrens *et al*., 1985).

Intracellular glutathione was monitored by the production of the fluorescent adduct, glutathionebimane (GSB) (Kosower and Kosower, 1987) as a result of the reaction of the cell permeant monochlorobimane (MCB, 50 μ$_M$) with reduced glutathione (GSH) catalysed by glutathione-S-transferase. Reduced nicotinamide nucleotides were monitored by their autofluorescence under the imaging conditions optimized previously (Aon *et al*., 2003; 2004). Experiments with cyanide (an in-hibitor of the electron transport chain) and the protonophore FCCP (carbonylcyanide-*p*-trifluoromethoxyphenylhydrazone) demonstrated that redox changes of nicotinamide nucleotides can be reliably monitored by autofluorescence. Fluorescence intensities were quantified by outlining mitochondrial compartment profiles (using TMRE fluorescence images) and counting pixel intensity distributions on a cell-by-cell basis (Aon *et al*., 2007a).

Analysis of apoptotic and necrotic cells

Cell death was analysed using Alexa Fluor 488 annexin-V/propidium iodide (Vybrant Apoptosis Assay Kit No. 2, Molecular Probes). The Alexa Fluor 488 conjugated to annexin-V interacts with externalized phosphatidyl-serine in apoptotic cells, producing a bright green

fluorescence, whereas necrotic cells are stained red by propidium iodide, which is impermeable to living cells.

Digestion of the cell walls to form spheroplasts was achieved by incubating the cells in an enzyme cocktail modified from Phillips *et al.* (2003). Cultured cells were harvested by centrifugation ($2000 \times g$) and washed twice in PBS, pH 5.6, before resuspension in 0.5 ml predigestion buffer (50 m$_M$ K$_2$HPO$_4$/5 m$_M$ EDTA/50 m$_M$ DTT, pH 7.2) for 30 min at 30 °C. Digestion of the cell wall was achieved at 30 °C after resuspending the cells in 0.5 ml digestion solution containing 50 m$_M$ KH$_2$PO$_4$/40 m$_M$ 2-mercaptoethanol/3 μg/ml chitinase/1.8 μg/ml lyticase (stock 200-1000 units/g)/12 μl *β*-glucuronidase/20 μl glusulase (Perkin-Elmer, Bucks, UK) in 2.4 $_M$ sorbitol, pH 7.2. Control cells were incubated for 30 min, whereas those exposed with any challenge agent were only digested for 20 min. Protoplasts were washed in modified annexin-binding buffer (MABB: 1.2 $_M$ sorbitol/10 m$_M$ Hepes/NaOH/40 m$_M$ NaCl/50 m$_M$ CaCl$_2$, pH 7.4). Annexin-V binding assays were performed according to the protocol of Madeo *et al.* (2002b) in MABB and 20 μl/ml annexin reagent preloaded and incubated at room temperature in the absence of light for 15 min. Spheroplasts were centrifuged at $1700 \times g$ and washed in MABB before 20 μg/ml PI was added.

Image acquisition and analysis

Images were recorded using a two-photon laser scanning microscope (Bio-Rad MRC-1024MP) with excitation at 740 nm (Tsunami Ti : Sapphire laser, Spectra-Physics) as described previously (Aon *et al.*, 2003). Owing to overlap in the crosssections for two-photon excitation of the three fluorophores of interest (Xu *et al.*, 1996; TMRE, CM-DCF, and NADH or GSB), this wavelength permitted recording of $\Delta\Psi_m$, ROS production and NAD(P)H (or GSH) simultaneously. The red emission of TMRE was collected at 605 ± 25 nm; the green emission of CM-DCF was recorded at 525 ± 25 nm; and the blue emission of GSB detected at 480 ± 20 nm. NADH emission was collected as the total fluorescence < 490 nm. At 3.5 s or 30 s intervals, as indicated, 512×512 pixel eight-bit greyscale images of the three emission channels were collected simultaneously and stored.

While measuring the kinetics of GSB production in cells, about 10 images were recorded to get the cellular background of NADH before addition of 50 μ$_M$ MCB. This was necessary because the NAD(P)H and GSB emissions were collected at similar wavelengths (i.e. 480-490 nm; Cortassa *et al.*, 2004; Aon *et al.*, 2007b). At steady state, the NAD(P)H fluorescence levels ($n = 14$) represented $31 \pm 1.2\%$ of the maximal GSB fluorescence levels attained ($n = 14$), indicating that GSB fluorescence was ~three-fold higher than the autofluorescence background. Images were analysed offline, using ImageJ software (Wayne Rasband, National Institutes of Health: http://rsb.info.nih.gov/ij/).

Fluorometric kinetic studies

The effect of DADS as a function of GSH concentration was further investigated using purified glutathione-S-transferase (GST, from equine liver; Sigma Aldrich, G6511) and GSH. Increasing concentrations of GSH (in PBS, pH 5.6) in the absence and presence of DADS (0.5 m$_M$/1.0 m$_M$) was added to 3 ml PBS, pH 5.6; a subsequent addition of 50 μl GST was used to initiate the reaction. Monochlorobimane (MCB, 2 μ$_M$ final concentration; Ex. = 391 nm, Em. = 491 nm) was used as previously described (Kosower and Kosower, 1987; Cortassa *et al.*, 2004) and fluorescence measured using a Cary Eclipse Fluorescence Spectrophotometer (Varian, Victoria, Australia). Nonlinear regression analysis of the GST kinetic data was performed, using a Levenberg-Marquardt algorithm (Microcal™ Origin, Northampton, MA).

Respiration measurements

Whole cells—Oxygen uptake was measured in organisms from exponentially growing cultures of *C. albicans*, using a closed electrode (Rank, Bottisham, Cambridge, UK) at 25 °C; after harvesting (2 min, $1000 \times g$), they were washed twice and resuspended in PBS at pH 5.2. Inhibitors/uncoupler were dissolved in ethanol and final solvent concentration in incubation mixture was <0.5%. IC_{50} values for AA, GP and DADS were determined using this technique.

Isolated mitochondria—*C. albicans w*as grown in yeast extract medium containing 2% glycerol. Cells were harvested from mid-exponential or stationary phase (after 24 h growth). Cell pellets were washed twice in PBS, pH 6.4, and suspended in an ice-cold isolation buffer (1.4 M sorbitol/50 mM K_2HPO_4/10 mM $MgCl_2$/1 mM EGTA). The cell suspension was disrupted in a Braun homogenizer using 0.4 mm diameter acid-washed glass beads for 2×1 min intervals, interspersed by cooling on ice (1 : 1:1 beads : cell suspension : free-space). The homogenate was centrifuged at 5000 r.p.m. for 5 min at 4 °C to remove whole cells and the remaining glass beads. The supernatant was further centrifuged at 10000 r.p.m. at 4 °C for 20 min to harvest the mitochondria. The pellet (mitochondria) was gently resuspended and washed in ice-cold isolation buffer, prior to final harvesting (1000 r.p.m./4 °C/20 min) and resuspension in ice-cold isolation buffer. The mitochondrial pellet was further analysed by electron microscopy (Lloyd *et al*., 2002). Isolated mitochondrial suspensions (50 μl) were incubated in a closed electrode system (Rank) containing 4 ml PBS at 30 °C for measurements of respiration. Oxygen consumption was measured using 10 mM potassium succinate and ADP was used at a final concentration of 10 mM to ensure that phosphorylation was maintained throughout the entire duration of the experiment.

ATPase activity

ATPase was assayed by proton release measured on adding cell-free extract to a stirred buffer (10 mM Tris/H_2SO_4/4 mM ATP/6 mM $MgSO_4$), pH 6.9, at 25 °C. A trace of carbonic anhydrase prevented drift of pH caused by absorption of atmospheric CO_2. An EIL combination pH-electrode connected to a Johnson Foundation pH-meter monitored the decreasing pH in the reaction mixture (total volume 2 ml). The output of the meter was connected via an amplifier to a 50 mV potentiometric recorder. Calibration was by adding known volumes of 100 mM HCl (Lloyd and Edwards, 1976).

Statistical analysis

Data were analysed using the software GraphPad Prism (version 2; San Diego, CA, USA). The statistical significance of the differences between treatments presented as mean $\pm$ SEM (95% confidence interval) was evaluated using a *t*-test (small samples, unpaired *t*-test with two-tail *p* values). The normality of the data was tested using the Kolmogorov-Smirnov test (GraphPad Prism).

Results

Compounds that affect the intracellular thiol redox balance are known to trigger oxidative stress. DADS, present in the garlic extract, is a potential thiol oxidant able to influence the thiol: disulphide redox potential and, through this, numerous cellular functions. Preliminary experiments showed that DADS triggered oxidative stress in either stationary or exponential phase cultures of *C. albicans*. Thus, we investigated the potentially deadly effects of DADS on this pathogen.

Cell death triggered by DADS

We exposed cells, harvested from early stationary phase of *C. albicans* cultures, transiently (30 min) to 0.5 m$_M$ DADS and investigated its effect on cell death. The kinetics of the appearance of apoptotic and necrotic cells was followed for up to 6 h after the short exposure to DADS (Figure 1). These studies were performed using two-photon laser scanning microscopy to record the binding of phosphatidylserine (PS), as an early apoptotic marker, and propidium iodide (PI), as a marker of non-viable (necrotic) cells (Figure 1B). Total cell numbers were counted in the channel measuring NAD(P)H fluorescence.

An immediate net increase of 11% in the number of necrotic cells, but not apoptotic cells, was observed during the transient 30 min exposure to 0.5 m$_M$ DADS. The percentage of necrotic cells increased to 50% within the next 2 h in the absence of DADS and was paralleled by a significant cell engagement in apoptosis at 2 h (20%), and even further at 4 h (33%) (Figure 1A), as could be judged by the bright green peripheral fluorescence of PS (Figure 1B).

Early intracellular events triggered by garlic components

Exposure of *C. albicans* to 0.5 m$_M$ DADS triggered rapid intracellular processes even before the cells exhibited substantial apoptosis or necrosis (Figure 1). We monitored key intracellular variables such as $\Delta\Psi$m, ROS (Figure 2A, B) and GSH (Figure 3), with TMRE, CM-DCF and MCB fluorescent probes, respectively, whereas the NAD(P)H redox status was imaged as cell autofluorescence (Figure 2C). Quantification of the steady-state signal from each fluorescent probe (as the mean intensity of cell fluorescence) is illustrated in Figure 4. When *C. albicans* cultures in early stationary phase were treated with 0.5 m$_M$ DADS, a pattern of effects characteristic of oxidative stress was induced, i.e. high ROS, low GSH and a decrease in NAD(P)H (Figures 2-4); a similar response was observed in exponential-phase cells (not shown).

Low levels of ROS, indicated by CM-DCF fluorescence, were detected in the mitochondria of control cells (Figure 2B). Treatment with DADS increased CM-DCF fluorescence in both the mitochondrial and cytoplasmic compartments (Figure 2B).

The formation of the glutathione-S-bimane product (GSB) was used to monitor GSH levels: this signal decreased significantly in the presence of DADS (Figures 3B, 4B). GSB appeared to be rapidly translocated to the vacuolar compartment, where it accumulated (Figure 3A).

After verifying that DADS did not influence MCB loading of the cells, we studied the effects of DADS addition on GSB fluorescence. When the MCB uptake reached a plateau (15 min loading with 40 μ_M MCB; see Figure 3A), we acutely added 0.5 m$_M$ DADS. Whole-cell GSB fluorescence was significantly reduced by 27% within 5 min (Figure 3B) and by 57% after 30 min of DADS treatment (Figure 4B). We have determined that at least one-third of the GSB fluorescence corresponds to NAD(P)H (see Materials and methods) and that both pools are decreased by DADS (Figures 3-5). Thus, at least one-third of the initial 5 min decrease in GSB fluorescence could be due to NAD(P)H oxidation.

IC$_{50}$ values for AA (Lemar *et al.*, 2005) and GP (Lemar *et al.*, 2002) were determined as 1 m$_M$ and 5 mg/ml, respectively. The IC$_{50}$ value for DADS (0.5 m$_M$) was determined by sequential addition to cells in the O$_2$ uptake assay.

A dramatic and significant increase in TMRE fluorescence of approximately three-fold was evident after treatment with DADS, as compared to controls or exposure to 1.0 m$_M$ AA or 5 mg/ml GP (Figure 4A). This increase in TMRE fluorescence was unexpected, since by all other variables, DADS induced oxidative stress concomitant with NAD(P)H and GSH oxidation, reflecting a generalized de-energization of the cells. Hence, we investigated whether the increase in TMRE fluorescence could have been due to dequenching of the dye as it is lost

from the mitochondrial matrix in association with ΔΨm depolarization, as described previously for cell loading with higher TMRE concentrations (Duchen *et al*., 1998). Thus, we tested whether a similar change in fluorescence was observed when we incubated yeast in the presence of 1 or 10 μM TMRE in the absence or presence of 0.5 mM DADS (not shown). We found that 0.5 mM DADS (for 1 h) induced a 1.85- and 2.17- fold increase in TMRE fluorescence by dequenching at 1 or 10 μM dye concentrations, respectively, at the level of individual mitochondria ($n = 35$; $p < 0.0001$), confirming that it was inducing $\Delta\Psi_m$ depolarization.

For comparison, the effects of GP and AA, another component of the garlic mixture, are shown for all cellular variables measured. As compared to DADS, the effects of GP and AA were less significant in all cases.

Effects of DADS on the intracellular redox environment

The pattern of cellular effects produced by DADS suggested that the increased oxidative stress was likely decreasing the redox potential of *Candida*. We further characterized this action of DADS through quantification of NAD(P)H.

Initially, we observed that the autofluorescence of mitochondrial NAD(P)H was intense in control samples, but this signal was attenuated by oxidation after addition of DADS (Figure 2C). Moreover, DADS decreased the GSB fluorescence (16 ± 0.7, $n = 10$) below the levels of NAD(P)H autofluorescence control (35 ± 0.9, $n = 14$), suggesting that the latter was also being diminished by DADS. After DADS addition, a very significant decrease in NAD(P)H could be observed in both the cytoplasmic and mitochondrial compartments (Figure 5).

Intracellular targets of DADS

Effects on glutathione S-transferase (GST)—GST catalyses the conversion of MCB and GSH to the fluorescent adduct GSB. In cells, this conversion takes place within minutes, and was accompanied by rapid translocation of GSB to vacuoles (Figure 3A). Fluorometric analysis of enzyme kinetics measured with the purified enzyme was used to establish whether GST (Sigma Aldrich, G6511) could be a target of DADS. Inhibition of GST was evident with increasing concentrations of DADS up to 10 mM. The GST Vmax was decreased 40% or 49% in the presence or 0.5 or 1.0 mM DADS, respectively [control, V_{max} (mM/ min) = 119.9; K_m (mM) = 3.85 ($r = 0.99$); 0.5 mM DADS, $V_{max} = 71.8$; $K_m = 3.85$ ($r = 0.99$); 1.0 mM DADS, $V_{max} = 59.3$; $K_m = 3.85$ ($r = 0.99$). Similar fluorimetric experiments performed in a cuvette demonstrated that DADS does not oxidize GSH itself directly (results not shown). Taken together, these results suggest that GST is at least one of the intracellular targets of DADS.

Effects on mitochondrial respiration—The rapid and significant $\Delta\Psi_m$ depolarization induced by DADS (see Figure 4A and text, above) suggested that mitochondrial respiration should also be affected. In whole organisms, addition of 10 mM glucose stimulated endogenous O_2 consumption by 22% (Figure 6a, b). DADS inhibited respiration, and this effect was not relieved by the respiratory uncoupler CCCP (Figure 6b, c).

The mitochondrial ATP synthase was also shown to be a target of DADS, since its activity was inhibited by 0.5 mM DADS in cell-free extracts ($IC_{50} = 5.3$ nmoles/mg protein). Oligomycin (5 μM; a well-known inhibitor of ATP synthase) was less potent than DADS ($IC_{50} = 16.5$ nmoles/mg protein).

The fact that CCCP was unable to uncouple respiration in whole cells in the presence of DADS pointed out that another site of action of the thiol oxidant was upstream of the ATP synthase. Further investigation of the site of DADS action in the respiratory chain of isolated mitochondria showed that DADS inhibited succinate-driven respiration (Figure 6B). These

results suggest that DADS affects at least one other site of the electron transport chain localized between complexes II-IV.

Discussion

We show here that DADS, a component of garlic powder, produced cell death in a high percentage of the *C. albicans* population. More importantly, the highly effective action of DADS on *C. albicans* was manifested as a long-term effect (2-4 h) after a relatively short (30 min) time exposure (Figure 1).

Glutathione depletion and increased oxidative stress in *C. albicans* treated with DADS

Early on during the 30 min treatment with DADS, several intracellular processes related to oxidative stress were activated. Concomitant with a generalized and significant increase in ROS production, glutathione was depleted and the NAD(P)H pool was oxidized after treatment with DADS (Figures 2-4). It appears that at least part of the decrease in the fluorescent adduct (GSB) associated with the GSH probe could be due to inhibition of glutathione-S-transferase by DADS.

The antioxidant defences of *C. albicans* are considered paramount for this organism to exhibit full virulence and to resist the host immune response. Thus, GSH is thought to play a role in the ability of this pathogen to defend itself against ROS and grow in the host successfully. Strong support for this idea originated from research carried out on auxotrophic mutants of *C. albicans* for GSH (Baek *et al*., 2004). Mutants of *C. albicans* for glutamylcysteine synthetase (GCS1), an essential enzyme in GSH synthesis, are sensitized to undergo apoptosis upon GSH depletion. Our results are in agreement with these results and strongly support the suggestion that a transient depletion of the GSH pool is sufficient to trigger the death process in *C. albicans*.

Mechanism of inhibition of mitochondrial respiration by DADS

Mitochondrial damage is likely to play a pivotal role in the cell death decision. ROS generation by mitochondria (a major site of free radical generation), in balance with the local anti-oxidant systems (e.g. GSH, SOD), determine a wide variety of biological functions, including apoptosis. Altered redox state, mitochondrial respiratory chain inhibition and loss of $\Delta\Psi_m$ are prominent features of various garlic constituents. Ajoene (20 μ_M), another chemical that can be isolated from garlic, is known to dissipate the $\Delta\Psi_m$ and activate caspases involved in programmed cell death in mammalian cells (Dirsch *et al*., 2002).

The oxidative stress observed in *C. albicans* after DADS treatment was paralleled by a marked decrease in $\Delta\Psi_m$ (Figures 2, 4), in agreement with previously reported data (Dirsch *et al*., 2002). A decrease of $\Delta\Psi_m$ is an early event initiated by oxidative stress (Richter, 1998). The ability of DADS to inhibit the respiration of cell suspensions prompted us to further investigate the targets in the mitochondrial respiratory chain, and we showed that DADS was able to inhibit succinate-driven respiration in isolated mitochondria (Figure 6). DADS may inhibit mitochondrial respiration at least at two different sites, the mitochondrial ATP synthase and the electron transport chain between complexes II and IV. Interestingly, DADS inhibition of the ATP synthase was even more potent than that of oligomycin. However, the observation that DADS inhibition of respiration in either whole cells or isolated mitochondria was not released by the uncoupler CCCP (Figure 6c, d, f), highlights the respiratory chain as another important target of DADS (Figure 6). An irreversible change in the oxidation status of critical cysteine residues of respiratory chain proteins may be responsible, as shown by previous studies (Gilbert, 1997,Helmerhorst *et al*., 2002,Schafer and Buettner, 2001). In the present study, we did not investigate whether or not DADS might also affect complex I in the respiratory chain.

Taken together, the data indicate that an early and generalized impairment of mitochondrial function is at the origin of cell death in *C. albicans*.

C. albicans death by necrosis and apoptosis following DADS treatment

The immediate necrotic response triggered by transient treatment with DADS in a *C. albicans* subpopulation, followed by a chronic apoptotic death of a large percentage of the cell population, is an important phenomenon (Figure 1). Particularly, the short exposure time and the low DADS concentration used (being removed thereafter) suggest its potential therapeutic value and also highlight the most sensitive intracellular targets of this dangerous opportunistic pathogen.

We suggest that the depletion of GSH is perhaps the more relevant determining factor in the candidicidal effects of DADS. As GSH is the major intracellular redox buffer in the organism, the ability to minimize oxidative stress is thereby diminished. The inability of mitochondria to remove these damaging free radicals would, therefore, result in their accumulation to above a threshold where continuing cell viability is impossible. Furthermore, as DADS induces a drastic oxidation of the mitochondrial NAD(P)H pool (Figures 2, 5), further reduction of GSSG by glutathione reductase is prevented, thus exacerbating the detrimental effect on the cell. In this scenario, the eventual route to death appears to be dependent on the concentration of the agent at the initial exposure.

Concluding remarks

Taken together, the results obtained strongly suggest that increased oxidative stress through decreased GSH levels mediate the drastic death response induced by DADS in *C. albicans*. Impairment of mitochondrial respiration, elicited by the action of DADS on ATPsynthase and a site located among complexes II-IV, also appear to be involved in the death response. In summary, we have described a promising therapeutic agent for *C. albicans*.

References

Aon MA, Cortassa S, Marban E, O'Rourke B. Synchronized whole cell oscillations in mitochondrial metabolism triggered by a local release of reactive oxygen species in cardiac myocytes. J Biol Chem 2003;278:44735–44744. [PubMed: 12930841]

Aon MA, Cortassa S, O'Rourke B. Percolation and criticality in a mitochondrial network. Proc Natl Acad Sci USA 2004;101:4447–4452. [PubMed: 15070738]

Aon MA, Cortassa S, Lemar KM, Hayes AJ, Lloyd D. Single and cell population oscillations in yeast: a two-photon scanning laser microscopy study. FEBS Lett 2007a;581:8–14. [PubMed: 17174310]

Aon MA, Cortassa S, Maack CH, O'Rourke B. Sequential opening of mitochondrial ion channels as a function of glutathione redox thiol status. J. Biol. Chem. 2007bin press

Baek YU, Kim YR, Yim HS, Kang SO. Disruption of γ-glutamylcysteine synthetase results in absolute glutathione auxotrophy and apoptosis in *Candida albicans*. FEBS Lett 2004;556:47–52. [PubMed: 14706824]

Bowen ID. Apoptosis or programmed cell death? Cell Biol Int 1993;17:365–380. [PubMed: 8318948]

Chance B, Sies H, Boveris A. Hydroperoxide metabolism in mammalian organs. Physiol Rev 1979;59:527–605. [PubMed: 37532]

Cortassa S, Aon MA, Winslow RL, O'Rourke B. A mitochondrial oscillator dependent on reactive oxygen species. Biophys J 2004;87:2060–2073. [PubMed: 15345581]

Cutler JE. Putative virulence factors of *Candida albicans*. Ann Rev Microbiol 1991;45:187–218. [PubMed: 1741614]

Del Carratore R, Della Croce C, Simili M, et al. Cell cycle and morphological alterations as indicative of apoptosis promoted by UV irradiation in *S. cerevisiae*. Mutat Res 2002;513:183–191. [PubMed: 11719103]

Dirsch VM, Antlsperger DS, Hentze H, Vollmar AM. Ajoene, an experimental anti-leukemic drug: mechanism of cell death. Leukemia 2002;16:74–83. [PubMed: 11840266]

Duchen MR, Leyssens A, Crompton M. Transient mitochondrial depolarizations reflect focal sarcoplasmic reticular calcium release in single rat cardiomyocytes. J Cell Biol 1998;142:975–988. [PubMed: 9722610]

Filomeni G, Aquilano K, Rotilio G, Ciriolo MR. Reactive oxygen species-dependent c-Jun NH2-terminal kinase/c-Jun signaling cascade mediates neuroblastoma cell death induced by diallyl disulfide. Cancer Res 2003;63:5940–5949. [PubMed: 14522920]

Frohlich K-U, Madeo F. Apoptosis in yeast: a monocellular organism exhibits altruistic behaviour. FEBS Lett 2000;473:6–9. [PubMed: 10802048]

Gilbert HF. Protein disulfide isomerase and assisted protein folding. J Biol Chem 1997;272:29399–29402. [PubMed: 9367991]

Halliwell, B.; Gutteridge, JMC. Free Radicals in Biology and Medicine. Oxford University Press; Oxford: 1999.

Harris JC, Plummer S, Turner MP, Lloyd D. The microaerophilic flagellate *Giardia intestinalis: Allium sativum* (garlic) is an effective antigiardial. Microbiology 2000;146:3119–3127. [PubMed: 11101670]

Helmerhorst EJ, Murphy MP, Troxler RF, Oppenheim FG. Characterization of the mitochondrial pathways in *Candida albicans*. Biochim Biophys Acta 2002;1556:73–80. [PubMed: 12351220]

Huh GH, Damsz B, Matsumoto TK, et al. Salt causes ion disequilibrium-induced programmed cell death in yeast and plants. Plant J 2002;29:649–659. [PubMed: 11874577]

Kosower NS, Kosower EM. Thiol labeling with bromobimanes. Methods Enzymol 1987;143:76–84. [PubMed: 3657564]

Laun P, Pichova A, Madeo F, et al. Aged yeast mother cells show markers of apoptosis. Sci World J 2001;1:141–146.

Lemar KM, Turner MP, Lloyd D. Garlic (*Allium sativum*) as an anti-*Candida* agent: a comparison of the efficacy of fresh garlic and freeze-dried extracts. J Appl Microbiol 2002;93:398–405. [PubMed: 12174037]

Lemar KM, Passa O, Aon MA, et al. Allyl alcohol and garlic (*Allium sativum*) extract produce oxidative stress in *Candida albicans*. Microbiology 2005;151:3257–3265. [PubMed: 16207909]

Lloyd D, Edwards SW. Mitochondrial adenosine triphosphatase of the fission yeast, *Schizosaccharomyces pombe* 972h⁻. Changes in activity and inhibitor-sensitivity in response to catabolite repression. Biochem J 1976;160:335–342. [PubMed: 12753]

Lloyd D, Salgado LE, Turner MP, Suller MT, Murray D. Cycles of mitochondrial energization driven by the ultradian clock in a continuous culture of *Saccharomyces cerevisiae*. Microbiology 2002;148:3715–3724. [PubMed: 12427961]

Loew LM, Tuft RA, Carrington W, Fay FS. Imaging in five dimensions: time-dependent membrane potentials in individual mitochondria. Biophys J 1993;65:2396–2407. [PubMed: 8312478]

Ludovico P, Sansonetty F, Corte-Real M. Assessment of mitochondrial membrane potential in yeast cell populations by flow cytometry. Microbiology 2001;147:3335–3343. [PubMed: 11739765]

Madeo F, Frohlich E, Frohlich KU. A yeast mutant showing diagnostic markers of early and late apoptosis. J Cell Biol 1997;139:729–734. [PubMed: 9348289]

Madeo F, Frohlich E, Ligr M, et al. Oxygen stress: a regulator of apoptosis in yeast. J Cell Biol 1999;145:757–767. [PubMed: 10330404]

Madeo F, Engelhardt S, Herker E, et al. Apoptosis in yeast: a new model system with applications in cell biology and medicine. Curr Genet 2002a;41:208–216. [PubMed: 12172961]

Madeo F, Herker E, Maldener C, et al. A caspase-related protease regulates apoptosis in yeast. Mol Cell 2002b;9:911–917. [PubMed: 11983181]

Odds, FC. Candida and Candidosis. Ballière-Tindall; London: 1988.

Park EK, Kwon KB, Park KI, Park BH, Jhee EC. Role of Ca^{2+} in diallyl disulfide-induced apoptotic cell death of HCT-15 cells. Exp Mol Med 2002;34:250–257. [PubMed: 12216118]

Phillips AJ, Sudbery I, Ramsdale M. Apoptosis induced by environmental stresses and amphotericin B in *Candida albicans*. Proc Natl Acad Sci USA 2003;100:14327–14332. [PubMed: 14623979]

Poljak A, Dawes IW, Ingelse BA, et al. Oxidative damage to proteins in yeast cells exposed to adaptive levels of H_2O_2. Redox Rep 2003;8:371–377. [PubMed: 14980070]

Reuter, HD.; Koch, HP.; Lawson, LD. Garlic: The Science and Therapeutic Application of Allium sativum and Related Species. Williams and Wilkins; Baltimore, MD: 1996.

Richter C. Nitric oxide and its congeners in mitochondria: implications for apoptosis. Environ Health Perspect 1998;106:1125–1130. [PubMed: 9788886]

Schafer FQ, Buettner GR. Redox environment of the cell as viewed through the redox state of the glutathione disulfide/glutathione couple. Free Radic Biol Med 2001;30:1191–1212. [PubMed: 11368918]

Schwartzman RA, Cidlowski JA. Apoptosis: the biochemistry and molecular biology of programmed cell death. Endocr Rev 1993;14:133–151. [PubMed: 8325248]

Severin FF, Hyman AA. Pheromone induces programmed cell death in *S. cerevisiae*. Curr Biol 2002;12:R233–235. [PubMed: 11937036]

Sundaram SG, Milner JA. Diallyl disulfide induces apoptosis of human colon tumor cells. Carcinogenesis 1996;17:669–673. [PubMed: 8625476]

Turrens JF, Alexandre A, Lehninger AL. Ubisemiquinone is the electron donor for superoxide formation by complex III of heart mitochondria. Arch Biochem Biophys 1985;237:408–414. [PubMed: 2983613]

Vanden Hoek TL, Shao Z, Li C, Schumacker PT, Becker LB. Mitochondrial electron transport can become a significant source of oxidative injury in cardiomyocytes. J Mol Cell Cardiol 1997;29:2441–2450. [PubMed: 9299367]

Willie AH. Glucocorticoid-induced thymocyte apoptosis is associated with endogenous endonuclease activation. Nature 1980;284:555–556. [PubMed: 6245367]

Xie Z, Kometiani P, Liu J, et al. Intracellular reactive oxygen species mediate the linkage of Na^+/K^+-ATPase to hypertrophy and its marker genes in cardiac myocytes. J Biol Chem 1999;274:19323–19328. [PubMed: 10383443]

Xu C, Zipfel W, Shear JB, Williams RM, Webb WW. Multiphoton fluorescence excitation: new spectral windows for biological nonlinear microscopy. Proc Natl Acad Sci USA 1996;20:10763–10768. [PubMed: 8855254]
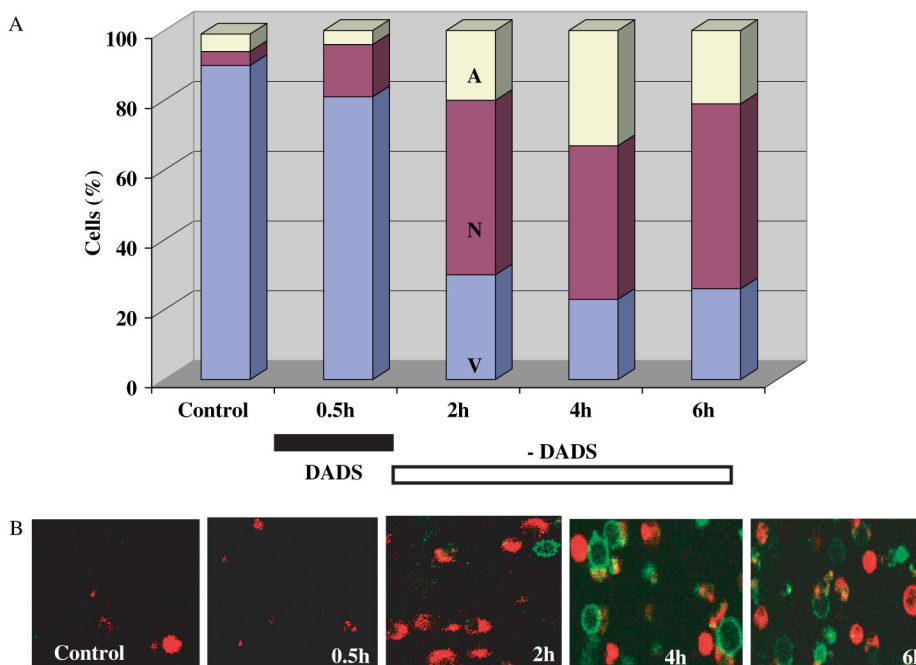
Figure 1.
Time course of cell death induction in *Candida albicans* after a short treatment with DADS.
(A) Culture-grown *C. albicans* cells were harvested in early stationary phase, as described in
Materials and methods, and exposed to 0.5 m$_M$ DADS for 30 min at room temperature, while
untreated cells remained as control. Cell death was monitored after DADS removal by sampling
at the times specified, in which the cells were washed and subjected to protoplasting, as
described in Materials and methods. Once protoplasted, the cells were resuspended in annexin-
binding buffer and incubated for at least 30 min with 10 μl Alexa Fluor 488 annexin V
(component A) and 5 μl propidium iodide (component B) from the Vybrant Apoptosis Assay
kit No. 2 (see Materials and methods), on coverslips coated with polylysine, in a thermostated
chamber at 30 °C, with unrestricted access to atmospheric oxygen on the stage of a Nikon
E600FN upright microscope. Total cell counts were 219, 272, 674, 504 and 771, respectively.
(B) Images of green and red fluorescence were recorded as described in Materials and methods.
Representative snapshots of the kinetics of appearance of necrotic (red) or apoptotic (green)
cells are shown. In all cases, cells viability and integrity was further tested by NAD(P)H
autofluorescence and transmitted light images from the same fields. A, apoptotic; N, necrotic;
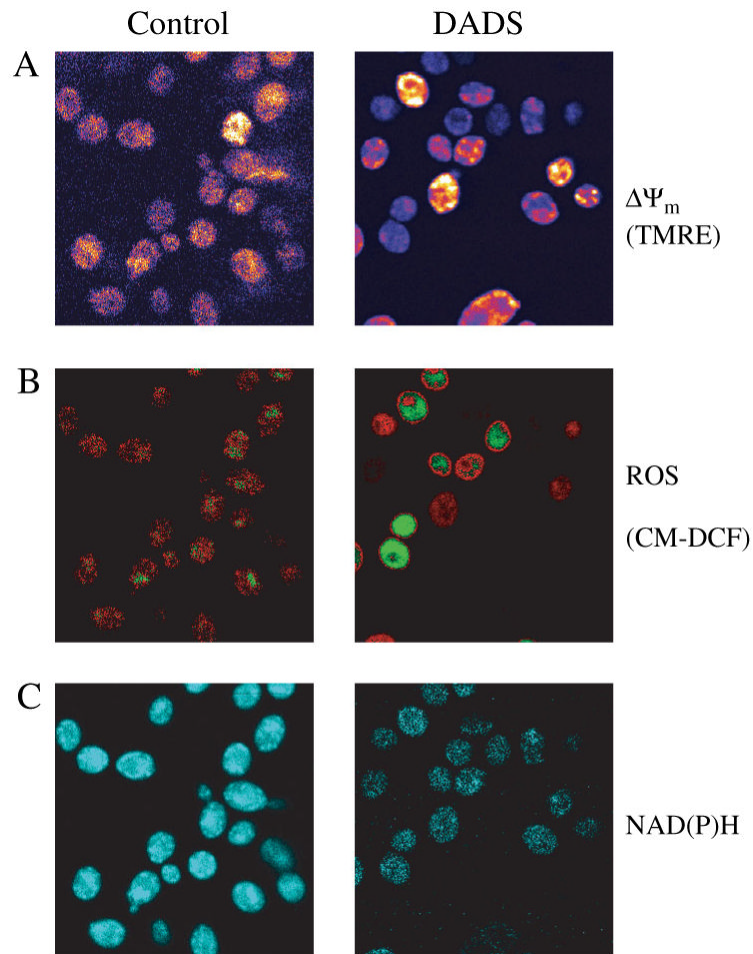V, viable; DADS, diallyl disulphide

Figure 2.
Fluorescent monitoring of $\Delta\Psi_m$, ROS and NAD(P)H from *C. albicans* with two-photon microscopy. Images of *C. albicans* early stationary phase cells were obtained as described in Materials and methods. Representative images of control and cells treated with 0.5 m$_M$ DADS after 30 min are shown. In TMRE-loaded yeast, the image of the control was 5× scaled up with respect to DADS-treated yeast (see text). All other signals are scaled comparably
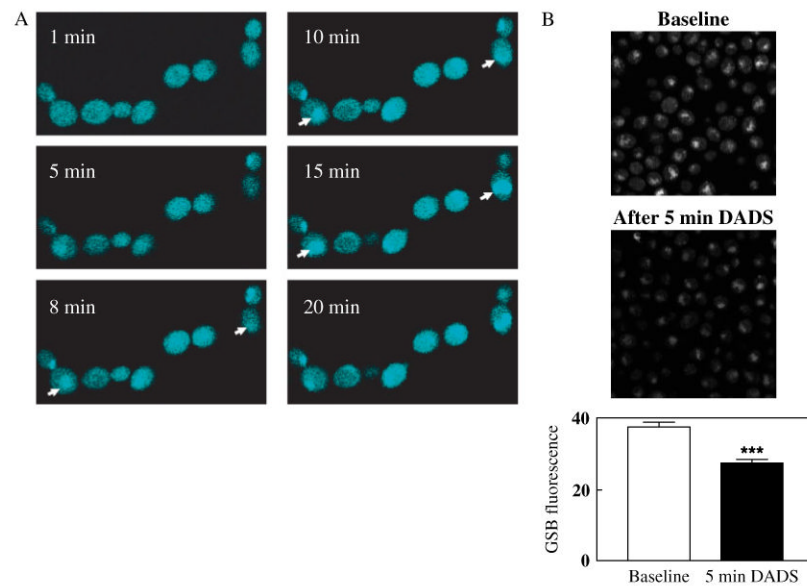
Figure 3.
Time course of GSB production in *C. albicans* and effects of DADS on MCB-loaded yeast.
(A) Cells harvested and processed as described in Materials and methods were loaded with 40
μ_M MCB by acute addition of the probe. Cells were imaged at the indicated times after MCB
addition in order to follow the kinetics of GSB production (cyan fluorescence). Arrowheads
indicate the progressive vacuolar localization of GSB. (B) Combined whole cell fluorescence
(mitochondrial, cytosolic and vacuolar) (bottom panels) was determined before (top panels)
and after 5 min exposure to 0.5 m_M DADS (middle panels) ($n = 20$; baseline = 37.5 ± 1.3 vs.
DADS after 5 min = 27.4 ± 1.0; $n = 20$, two independent experiments). ***$p < 0.001$
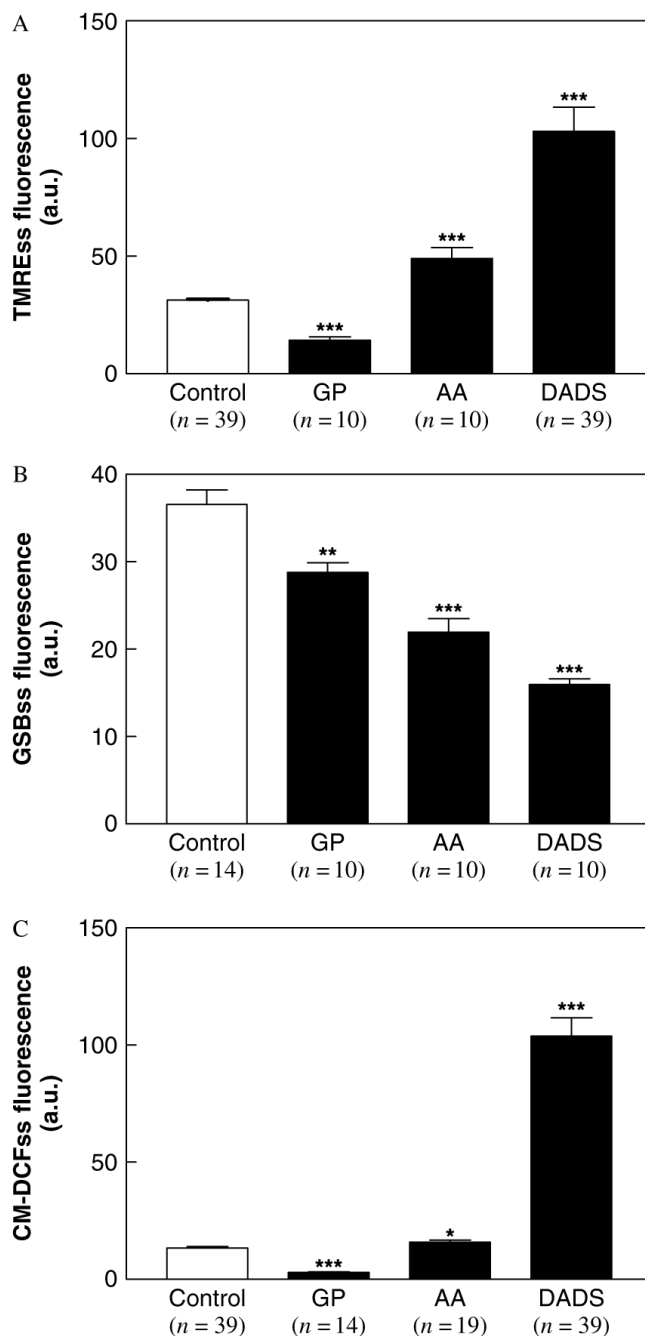
Figure 4.
Quantifying the effects of garlic components on different cellular variables from two-photon microscopy images. Culture-grown *C. albicans* cells were harvested in early stationary phase, as described in Materials and methods, and exposed to different garlic components at room temperature. The steady-state level of fluorescence (mean of maximal fluorescence intensity) from TMRE, GSB and CM-DCF probes were determined after 30 min treatment with 0.5 m$_M$ DADS, or 1.0 m$_M$ AA or 5 mg/ml GP. ***$p < 0.001$; **$p < 0.01$; *$p < 0.05$ vs. control. AA, allyl alcohol; GP, garlic powder
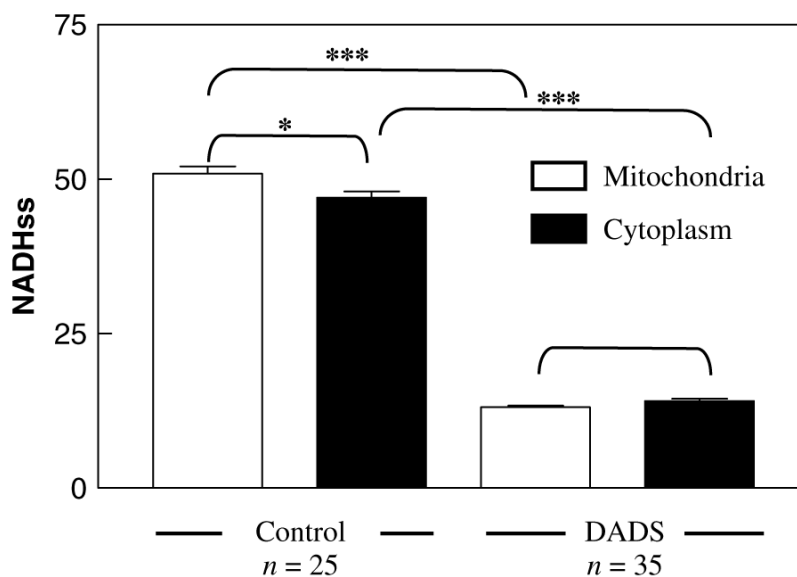
Figure 5.
Effect of DADS on the cellular redox environment. The intensities of NAD(P)H autofluorescence in mitochondrial and cytoplasmic compartments were determined in culture-grown *C. albicans* harvested in early stationary phase, as described in Materials and methods. Quantification was performed in cells in the absence (control) or presence of 0.5 m$_M$ DADS. Cells loaded with TMRE allowed determination of the regions of interest corresponding to mitochondria or cytoplasm, in order to quantify autofluorescence in both compartments. The brackets above the bars indicate the statistical significance corresponding to different compartments and/or the absence or presence of DADS. ***$p < 0.001$; *$p < 0.05$; no asterisk, $p > 0.05$
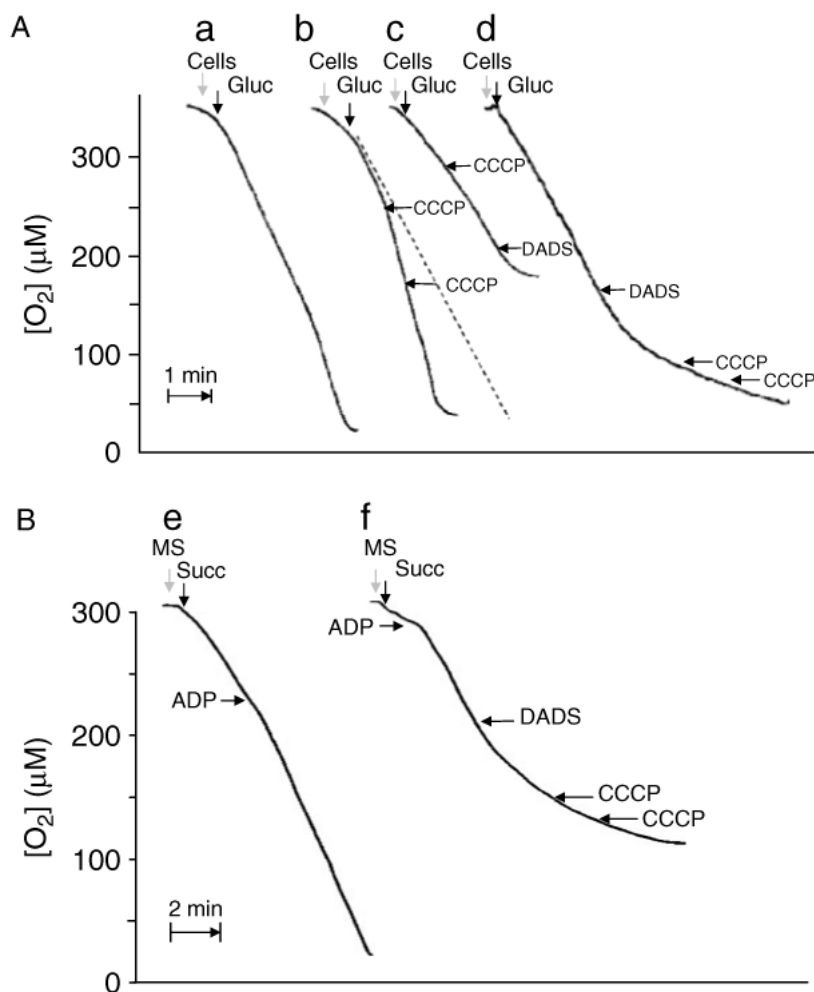
Figure 6.
Effect of DADS on mitochondrial respiration. (A) Oxygen consumption of organisms harvested from an exponentially growing culture of *C. albicans*. Grey arrow indicates addition of cells and black arrow indicates addition of 10 m$_M$ glucose. a, Control. b, Effect of the uncoupler CCCP (0.2 μg/ml added at each arrow); dotted line indicates glucose-driven respiration; percentage increase after addition of CCCP was 71%. c, The inhibitory effect (80%) of 1 m$_M$ DADS after addition of excess CCCP (1 μg/ml); further addition of CCCP did not release inhibition (results not shown). d, Effect of CCCP (0.1 μg/ml added at each arrow) on cells whose respiration was 80% inhibited by 1 m$_M$ DADS. (B) Mitochondrial respiration driven by 10 m$_M$ succinate (black vertical arrow) was measured as described in Materials and methods; 50 μl mitochondrial suspension was added at light grey arrow and 10 m$_M$ ADP was added at black horizontal arrow. Inhibitors were added as indicated: 1.0 m$_M$ DADS (80% inhibition) and 0.5 μ$_M$ CCCP (the uncoupler). Gluc, glucose; MS, mitochondrial suspension; Succ, succinate